JOURNAL OF AIRCRAFT
Vol. 44, No. 4, July–August 2007

Effect of Acoustic Slat Modifications on Aerodynamic Properties of High-Lift Systems

Judith Ortmann* and Jochen Wild*
DLR, German Aerospace Research Center, Braunschweig 38108, Germany

DOI: 10.2514/1.26307

The objective of this study is the determination of the effect of brushlike devices at the slat trailing edge on the aerodynamic properties of a high-lift system. Such devices have shown promising results with respect to significant noise reduction. But up to now, the effect of these devices on the aerodynamic properties has not been considered. This study shows that all investigated cylindrical brush hairs affect the aerodynamic properties of a high-lift system adversely, due to the influenced slat wake. But by cutting many small gaps into the slat trailing edge, resulting in brushes of rectangular cross section, the effect on the global coefficients is minor, sometimes slightly favorable.

Nomenclature

C_D	=	drag coefficient
C_L	=	lift coefficient
c_p	=	pressure coefficient
Ma	=	Mach number
Re	=	Reynolds number
y^+	=	dimensionless wall distance
$\bar{u}$, $\bar{v}$, $\bar{w}$	=	time-averaged flow velocity
u', v', w'	=	turbulent fluctuation velocities
$u(t)$, $v(t)$, $w(t)$	=	time components of the velocity

I. Introduction

DURING the approach flight of a modern transport aircraft, the slat trailing edge is known to be one major airframe noise source [1]. This is caused by the interaction of sharp edges with vortices in the turbulent boundary layer at high velocities at the slat trailing edge. To avoid the sharp edges, brushlike devices could be installed. By this, one would like to achieve a viscous damping of the turbulent fluctuation velocities u', v', and w', where

$$u' = u(t) - \bar{u} \tag{1}$$

Acoustic experiments with such devices at the sides of the slat and flap were successful (see Phelan [2]). Now, experiments with devices at the whole slat trailing edge have to be investigated. There is a European patent by Mau and Dobrzynski [3] for several noise-reduction devices on high-lift systems. First, cylindrical brush hairs were used because there are successful aeroacoustic tests with such devices installed on the trailing edge of a flat plate investigated by Herr and Dobrzynski [4] and their installation is relatively simple.

But for practical reasons, there is a step between the trailing edge of the slat and the cylindrical brush hairs. One possibility to avoid this step is the installation of brushes with a rectangular cross section. This can be obtained by cutting many small gaps into the slat trailing edge.

Up to now, there were only aeroacoustic tests with such brushlike devices at the slat trailing edge. The flow mechanism and the effect on the aerodynamic properties of a high-lift wing are unknown. This study will present and analyze the very complex flow in the area of the brush hairs and the effect on the high-lift flow.

Presented as Paper 3842 at the 24th AIAA Applied Aerodynamics Conference, San Francisco, CA, 5–8 June 2006; received 13 July 2006; revision received 30 January 2007; accepted for publication 30 January 2007.

*Research Engineer, Institute of Aerodynamics and Flow Technology, Lilienthalplatz 7.

II. Geometry

To obtain the effect of the brushlike devices at the blunt slat trailing edge on the aerodynamic properties of a high-lift system, the clean slat configuration is trimmed by the length of the brush hairs. At this thicker trailing edge, the brushes can be installed.

Because of computational resource limitations, the tiny brush hairs could not be simulated on the whole slat trailing edge of a transport aircraft. Therefore, a representative wing section of a high-lift wing is staggered with the leading-edge sweep angle to generate a small portion of an infinite swept wing of the same cross section (Figs. 1a and 1b). This way, only a few brush hairs have to be simulated. For the computation, the small section is extended infinitely by applying periodic boundary conditions. The brush hairs are arranged parallel to the incoming flow on the blunt slat trailing edge.

Similar to the setup of the acoustical tests, cylindrical brush hairs were installed (Fig. 1c) with a backwards-facing step in the area of the root of the brush hairs. These devices are represented by a stiff cylinder. Considering flexible cylinders requires the time-accurate, coupled simulation of the interaction of the structure and the aerodynamic flow. These computations are extremely costly and time-consuming and are therefore beyond the scope of the present work. In acoustic experiments, steel needles are also investigated, which presented brush hairs that were as stiff as possible. These needles can also reduce the trailing-edge noise (Fig. 2; results of acoustic experiments on the NACA-0012 profile). But up to now, no experimental investigations on the aerodynamic performance were made that can be used for a comparison with the results of this study.

To avoid the step at the root of the brushes, brush hairs with a rectangular cross section are preferred. This can be achieved by cutting small gaps into the slat trailing edge (Fig. 1d).

In addition to the two different shapes of the brushlike devices, the influence of length, diameter, and spacing on the high-lift performance are investigated in this study.

III. Grid Generation and Flow Solver

For the computation, a block-structured grid was generated with MegaCads [5], and the brush hairs were modeled with the chimera technique [6]. With this technique, the grid in the area of interest can be generated in an extra block (see Fig. 3). By cutting a hole in the main grid of the whole high-lift wing with the clean slat trailing edge, and using the chimera block over this hole, different slat trailing-edge modifications can be simulated, while the main grid stays the same for all investigated models. Both grids have to overlap for boundary data exchange. The total grid has about 2.5 M points. The number of points normal to the wall across the boundary layer of the global grid

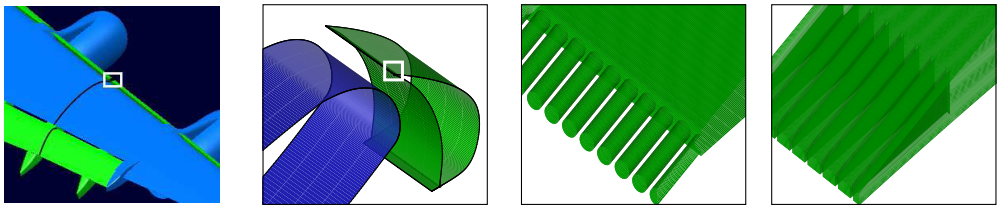

a) b) c) d)

Fig. 1 Slat system: a) profile position, b) swept 3-D section for RANS-simulation, c) slat trailing edge with cylindrical brush hairs, and d) brushes with rectangular cross section.

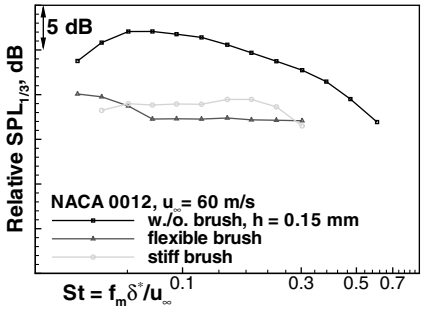

Fig. 2 Comparison of the noise-reducing potential of flexible and stiff brush hairs (with permission from Michaela Herr, DLR, German Aerospace Research Center, Braunschweig, Germany.)

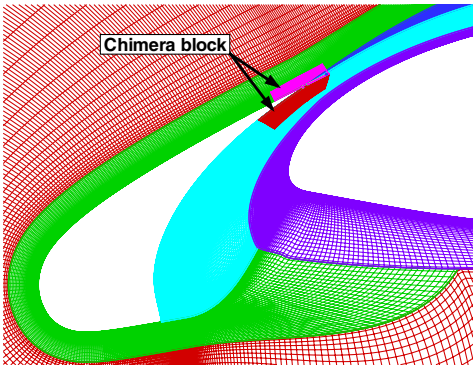

Fig. 3 Structured grid around the slat with the chimera block.

is 64 (even in the chimera block). Between the brush hairs, there are 16 points in spanwise direction. Thus, the grid is of high resolution.

For the global grid, y^+ is in the order of 1. Around the brush hairs, y^+ values even below 1 are realized.

By applying the flow solver FLOWer [7], the fully turbulent flow is investigated. FLOWer solves the Reynolds-averaged Navier–Stokes (RANS) equations using the Spalart–Allmaras turbulence model [8] with the Edwards–Chandra modification [9]. The finite volume method and the Runge–Kutta scheme for the time-stepping were used.

The wing section of the high-lift system was derived from a wind-tunnel model. Thus, the viscous flow was simulated with the following incoming flow conditions: 1) Mach number $Ma = 0.22$ and 2) Reynolds number $Re = 2.91 \times 10^6$.

To estimate the discretization error, a grid-convergence study was conducted [10]. It is shown that by using the grid of generated size, almost grid-independent solutions are obtained; thus, the discretization error is considered to be negligible.

IV. Results

For multi-element high-lift systems, all high-lift elements affect each other, and the main parameters are the gap and the overlap (see Smith [11]). The brushlike devices increase the effective gap and overlap between the slat and the main wing, due to their permeability. The associated influence on the overall lift coefficient is driven by the following two main effects:

1) The slat effect occurs when the circulation around an upstream wing element induces velocities at the leading edge of the downstream element that are directed against the local flow direction. These induced velocities decrease the suction peak of the downstream element.

2) The circulation effect occurs when the circulation around a downstream wing element induces velocity components normal to the trailing edge of the upstream element. Thus, the circulation around the forward element increases to comply with the Kutta condition.

Considering these effects, the changes of pressure distributions and force coefficients of the different brush devices can be explained.

A. Effect of Length, Thickness, and Spacing of the Cylindrical Brush Hairs

To investigate the influence of the cylindrical brush hairs, the length, diameter, and spacing of these devices are varied. First, the length is changed from case 1 with 0.24% of the cruise wing chord (reference length) to case 2 with about 0.52%. The diameter of both cases is 0.035% of the reference length and the spacing of the brushes is 25% of the brush diameter. In case 3, only the diameter increases to 0.053% of the reference length. The brush length stays the same as in case 2. The brush length of case 4 is 0.62% and the diameter is 0.07% of the reference length. Then, the spacing of cases 1 to 3 is reduced to exactly 5% (in the following small spacing) of the respective brush diameter. Additional analysis with a further reduction of the spacing to 1% of the brush diameter did not show improvements.

The complex flow topology around the cylindrical brush hairs is shown in Fig. 4. There is a vortex oriented perpendicular to the incoming flow. In addition, separation lines at the sides and an attachment line at the suction side of the brush hair can be seen (Fig. 4c). Additional analysis have also shown the occurrence of an attachment line at the pressure side. These flow features are typical for cylinders in skewed inflow.

In the Mach number distribution of a cut normal to the brushes (Fig. 5a), a strong acceleration between the brush hairs can be seen. If the spacing between the brush hairs is reduced to a certain extent, a

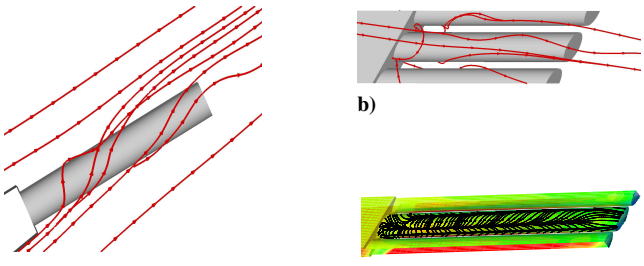

a) b) c)

Fig. 4 Flow topology of the cylindrical brush hairs shows complex vorticity: a) side view, b) top view, and c) surface pressure distribution with flow trajectories on the suction surface of the cylindrical brush hairs.

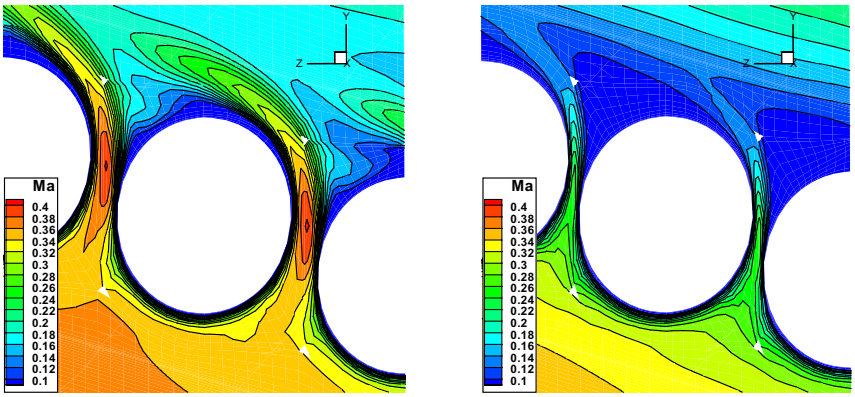

Fig. 5 Mach number distribution in a cut normal to the brush hairs: a) strong acceleration between the brush hairs and b) blockage between brush hairs with small spacing.

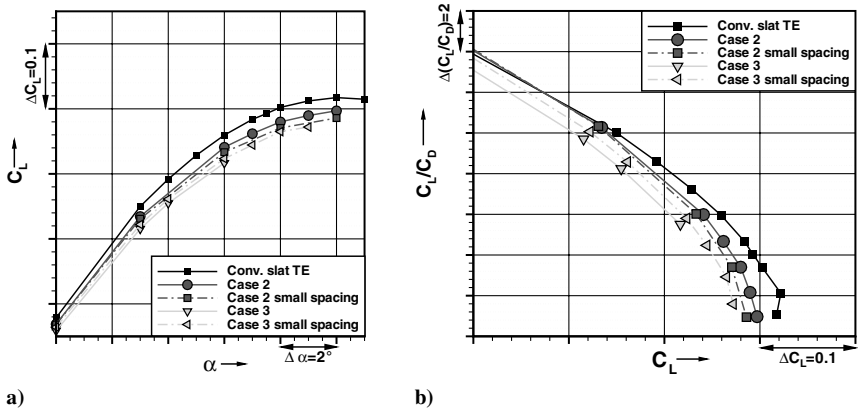

Fig. 6 The high-lift extract of the aerodynamic performance for different brush parameters (diameter times length and spacing): a) lift curve and b) lift-to-drag ratio.

blockage occurs, which is caused by the boundary layers of the brush hairs decelerating the flow.

The application of cylindrical brush hairs with large or small spacing reduces the global lift coefficient (Fig. 6a) and increases the global drag coefficient. The lift-to-drag ratio in the cases of high-lift decreases (Fig. 6b), especially with increasing length and diameter of the brush hairs.

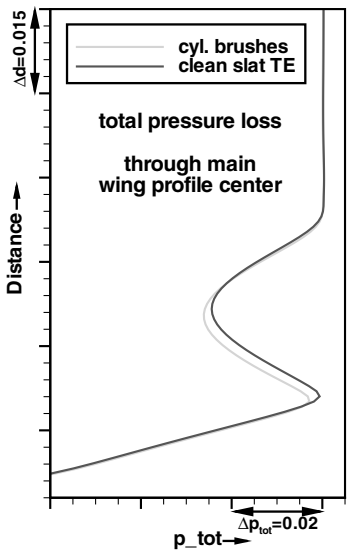

Fig. 7 Total pressure loss in a cut on the suction side through the center of the main wing profile.

Additional analyses have shown that the vortices caused by the brush hairs (especially the cross vortex at the brush root) significantly influence the flow and the circulation around the whole profile. The slat wake is wider and closer to the suction side of the main wing (Fig. 7) and interferes with its boundary layer farther upstream. In the boundary layer, the loss of momentum increases, reducing the circulation around the main wing. Particularly with increasing length of the brush hairs, the slat trailing-edge pressure rises because of the circulation effect (Fig. 8a). The velocities at the slat trailing edge decrease, and the suction peaks and suction levels are reduced (Figs. 8b and 8c). Consequently, the lift coefficient declines for all high-lift elements (Fig. 9, left) and, thus, so does the global lift coefficient.

For the contribution to the drag coefficient, the pressure-induced part is dominating, thus, the slat drag is now dominant (Fig. 9, right).

The blockage of the brush hairs with the small spacing reduces the velocity between the brushes. As a consequence, the slat trailing-edge pressure increases less than in the previous case with the larger spacing (Fig. 10a). The suction peak and its contribution to the lift coefficient increases. In this case, the slat effect is dominating, and so the suction peak at the main wing (Fig. 10b) and its contribution to the lift coefficient is reduced. The same holds for the brushes with large spacing. At the flap, the spacing effect is barely noticeable (Fig. 10c). The pressure-induced part of the drag coefficient of the slat is minor and rises at the main wing.

To investigate the influence of the changed effective gap and overlap (caused by the brush spacing), a setting variation of the slat position is done. The slat is shifted separately in the x and y directions. With increasing distance between the slat and main wing, the lift coefficient rises (Fig. 11), but the drag coefficient also decreases for all shifted positions. Without an investigation of the

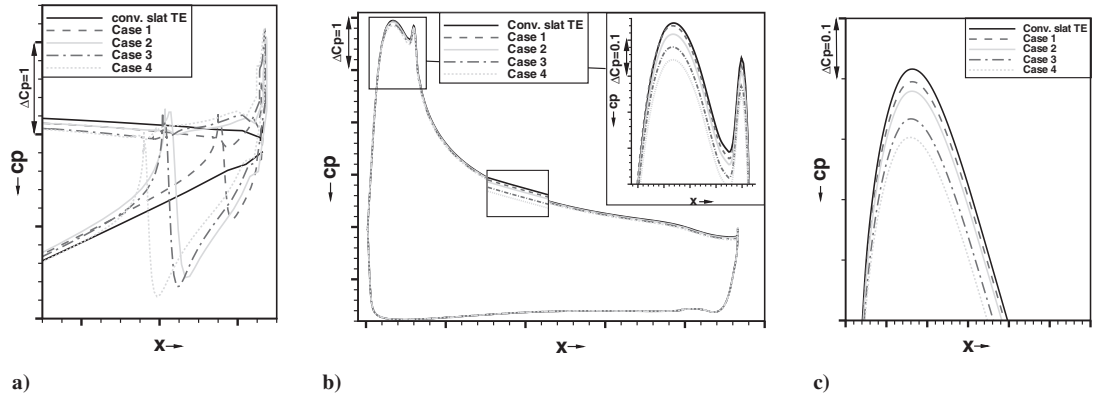

a) b) c)

Fig. 8 Influence of brush hair diameter and length: a) pressure distribution on the slat trailing edge (cut through the middle of the brush), b) over the main wing, and c) on the pressure peak of the flap.

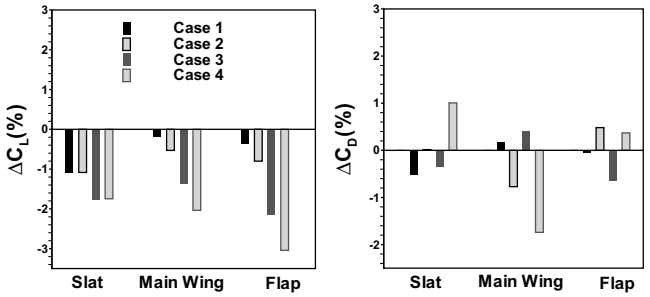

Fig. 9 Forces of the wing elements relative to the clean slat configuration; influence of the brush diameter and length (initial space).

moment coefficients, no clear conclusion about compensating for the loss of performance by optimizing the slat position can be drawn.

B. Effect of Shape: Cylindrical vs Rectangular Brush Hairs

The mostly negative effect of the cylindrical brush hairs is caused by the step in the area of the root of the brush hairs. Because, here, a vortex perpendicular is generated to the incoming flow. Thus, the interaction between the slat wake and the boundary layer of the main wing happens farther upstream and decreases the aerodynamic performance.

Brushes with rectangular cross section can have a smooth transition from the slat trailing edge to the brush hairs. A second advantage of the rectangular brushes is the decreasing height of the gap with constant width between the brush hairs toward their end. This way, the discharge flow rate can increase from the root to the end of the brush.

The flow topology of the brush hairs with rectangular cross section (Fig. 12) shows that there is no cross vortex now and the turbulence caused by the brush hairs is lower. Also, the blockage of this type of brush hair is stronger (Fig. 13). Thereby, the influences of the brush hairs on the slat wake (Fig. 14) and on the loss of momentum are reduced.

The global lift coefficient of the brushes with rectangular cross section is comparable to the clean slat configuration (Fig. 15a). Also, the lift-to-drag ratio for the high-lift is of same order of magnitude (Fig. 15b). In case 1 (the tiniest investigated brush hairs), the lift-to-drag ratio even increases. This can be explain by the changed effective gap and overlap of the slat and the main wing. The slat position is probably not an optimal approach configuration. The slightly larger brush hairs influence the aerodynamic performance even more. Thus, the lift-to-drag ratio decreases, but it is still of the same order as for the clean slat configuration.

Because of the stronger blockage, the differences of the pressure at the slat trailing edge decreases (Fig. 16a) and the circulation around the total configuration rises. The suction peak of all high-lift elements increases (Figs. 16b and 16c) because of the dominating circulation effect.

Because of the significant reduction of the pressure differences at the slat trailing edge, the slat lift coefficient decreases (Fig. 17, left), although the slat suction peak rises slightly. The suction level of the total main wing and the flap increases and so does their contribution to the lift coefficient. The pressure-induced part of the slat drag coefficient grows (Fig. 17, right), caused by the decreasing local lift coefficient. Because of the minor loss of momentum at the main wing, the drag coefficient is reduced. The slat wake does not affect the flow around the flap, although the pressure-induced drag coefficient of the flap increases because of the higher suction level.

V. Conclusions

This study shows the very complex flow topology in the region of brush hairs applied to the trailing edge of a slat device and their

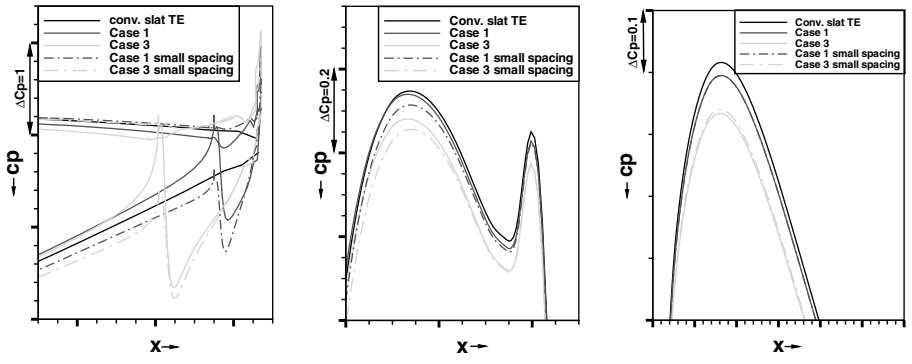

a) b) c)

Fig. 10 Influence of brush hair spacing: a) pressure distribution on the slat trailing edge (cut through the mid of the brush), b) on the main wing pressure peak, and c) on the flap pressure peak.

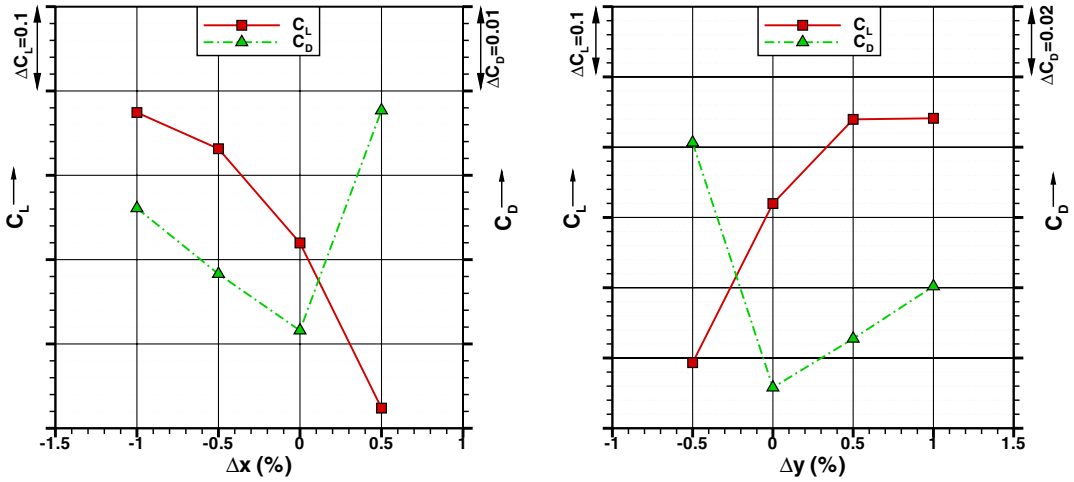

a) b)

Fig. 11 Influence of the slat position on C_L for case 2 (small space): a) shift in the x direction and b) shift in the y direction.

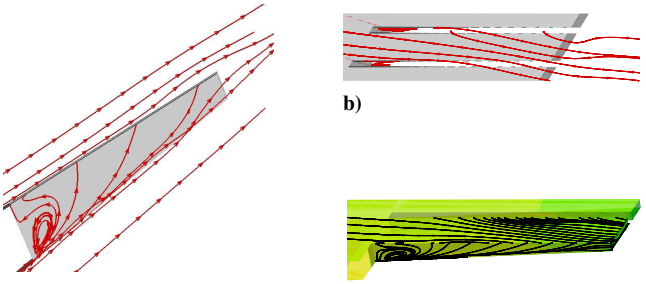

a) b) c)

Fig. 12 Flow topology of the brush hairs with rectangular cross section shows less vorticity than for the cylindrical brush hairs: a) side view, b) top view, and c) surface pressure distribution with surface flow trajectories of the brush hairs with rectangular cross section.

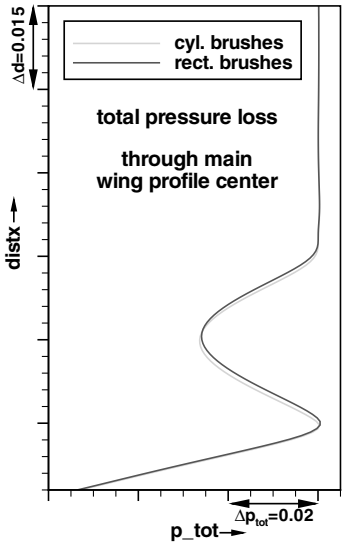

Fig. 14 Total pressure loss in a cut on the suction side through the center of the main wing profile.

influence on the aerodynamic properties of a high-lift system. All investigated cylindrical brush hairs affect the aerodynamic properties adversely, because of the step at the root of the brushes. The cross vortex at the brush root impairs the flow around the slat trailing edge. The slat wake is wider and closer to the suction side of the main wing and mixes with its boundary layer farther upstream. The aerodynamic performance degrades with increasing length and diameter of the brush hairs. A reduction of the spacing of the brushes barely recovers the aerodynamic performance of the clean slat device.

Brush hairs with rectangular cross section can have a smooth transition from slat trailing edge to the brushes and affect the flow insignificantly. The changes in the flow around the slat trailing edge are minor compared with the cylindrical brushes, and the slat wake is thinner. The adverse effect on the aerodynamic properties is significantly reduced. Also, the blockage of the brush hairs is larger and the pressure equalization increases from the brush root toward

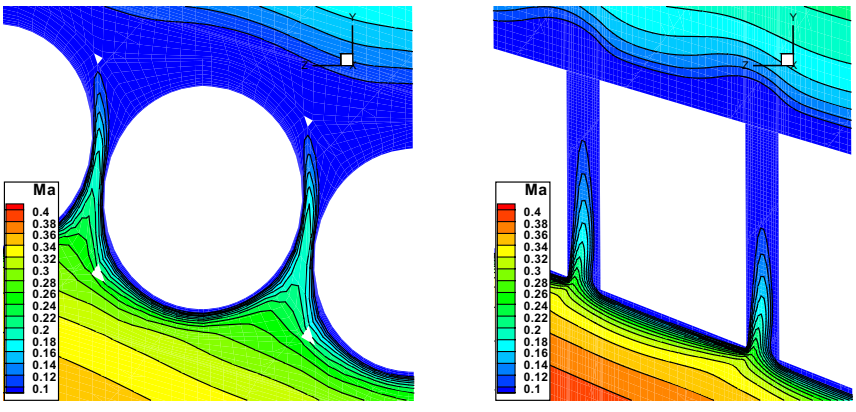

a) b)

Fig. 13 Mach number distribution in a cut normal to the brush hairs: a) blockage between the cylindrical brush hairs with the small spacing (5% of the brush diameter) and b) stronger blockage between rectangular brush hairs with the same parameter as the cylindrical in Fig. 13a.

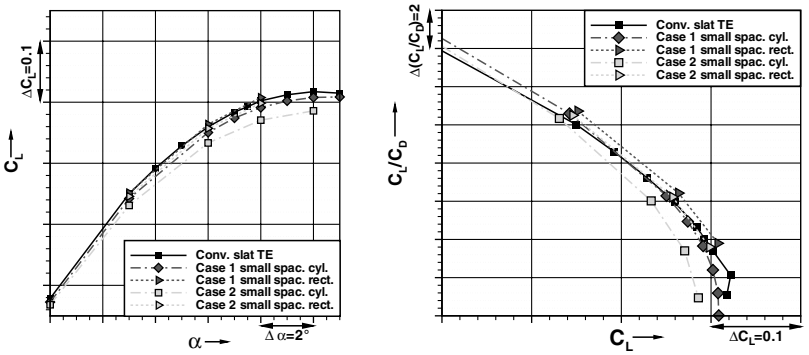

Fig. 15 The aerodynamic performance for different brush hair shapes (cylindrical vs rectangular): a) lift curve, b) lift-to-drag ratio.

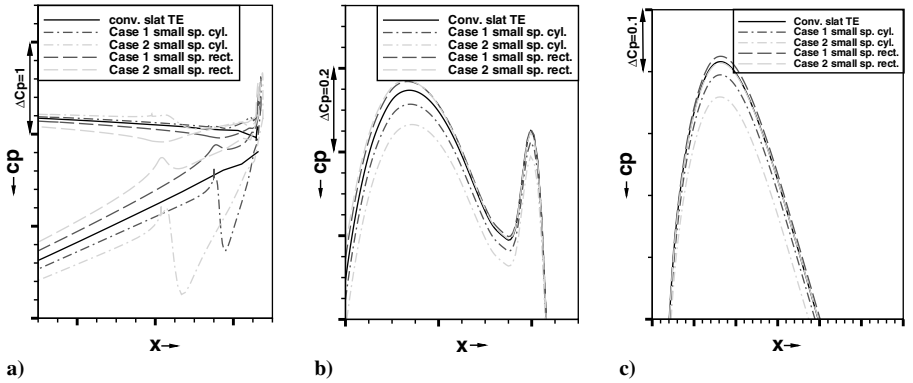

Fig. 16 Influence of the brush shape (cylindrical vs rectangular): a) pressure distribution on the slat trailing edge at the mid of the brush, b) on the main wing pressure peak, and c) on the flap pressure peak.

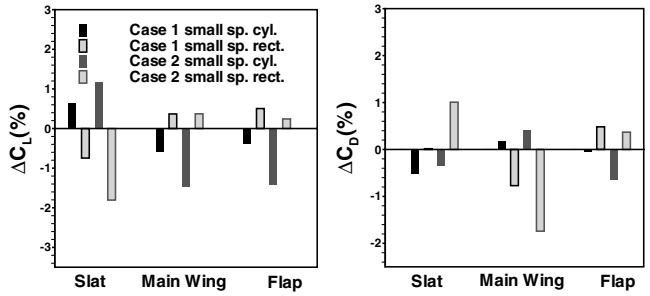

Fig. 17 Forces of the wing elements relative to the clean slat configuration; influence of the brush shape (cylindrical vs rectangular).

their end. The loss of lift is insignificantly smaller than for the cylindrical brush hairs.

This study shows that from the aerodynamic point of view, the brush hairs with the rectangular cross section are the most promising devices. In the future, the brushes with rectangular cross section also have to be investigated in acoustic tests.

Acknowledgments

The authors would like to thank Jan W. Delfs and Michaela Herr for their explanations and support of the acoustical aspects.

References

[1] Dobrzynski, W., Nagakura, K, Gehlhar, B., and Buschbaum, A., "Airframe Noise Studies on Wings with Deployed High-Lift Devices," AIAA Paper 98-2337, 1998.

[2] Phelan, M., "Airbus Combs Airflow in Quest for Aircraft," *Flight International*, Vol. 164, Feb.–Mar. 2003, p. 24.

[3] Mau, K., and Dobrzynski, W., "Anordnung zur Minderung des Aerodynamischen Lärms an einem Vorflügel eines Verkehrsflugzeuges," German Patent 101 57 849, filed 2002; also European Patent EP 1 314 642 B1, filed 2005.

[4] Herr, M., and Dobrzynski, W., "Experimental Investigation in Low Noise Trailing Edge Design," AIAA Paper 2004-2804, 2004.

[5] Brodersen, O., Hepperle, M., Ronzheimer, A., Rossow, C. C., and Schöning, B., "The Parametric Grid Generation System MegaCads," *Numerical Grid Generation in Computational Field Simulations*, NSF Engineering Research Center, Mississippi State Univ., Mississippi State, MS, 1996, pp. 353–362.

[6] Schwarz, T., "The Overlapping Grid Technique for the Time Accurate Simulation of Rotorcraft Flows," 31st European Rotorcraft Forum, Florence, Italy, Associazione Italiana di Aeronautica e Astronautica, Paper 86, 2005.

[7] Kroll, N., Radespiel, R., and Rossow, C. C., "Structured Grid Solver 1: Accurate and Efficient Flow Solvers for 3D Applications on Structured Meshes," AGARD Rept. 807, 1995.

[8] Spalart, P. R., and Allmaras, S. R., "One-Equation Turbulence Model for Aerodynamic Flow," AIAA Paper 92-439, 1992.

[9] Edwards, J. R., and Chandra, S., "Comparison of Eddy Viscosity-Transport Turbulence Models for Three-Dimensional, Shock-Separated Flowfields," *AIAA Journal*, Vol. 34, No. 4, 1996, pp. 756–763.

[10] Ortmann, J., and Wild, J., "Effect of Noise Reducing Modifications of the Slat on Aerodynamic Properties of the High-Lift System," *Notes on Numerical Fluid Mechanics and Multidisciplinary Design*, Vol. 92, Springer–Verlag, Berlin, 2006, pp. 357–364.

[11] Smith, A. M. O., "High-Lift Aerodynamics (Wright Brothers Lecture)," *Journal of Aircraft*, Vol. 12, No. 6, 1975, pp. 501–530; also AIAA Paper 74-939, 1974.